Smelov M.V.

THEORETICAL AND EXPERIMENTAL INVESTIGATION OF THE PROPAGATION OF ELECTROMAGNETIC WAVES KNOTTED INDUCED IN THE ANTENNA FIELD KNOTTED ANECHOIC CONDITIONS

The article describes the results of theoretical and experimental studies on the spread of knotted electromagnetic waves induced in the antenna field knotted anechoic conditions. Knotted antenna is a linear phased array antenna (PAA), which consists of two elements in the form of knotted antennae, each in the form of cinquefoil.

The aim of theoretical research, using topological properties of Hopf of S^2 bundle in the sphere S^3 [1] to calculate explicitly function that describes the motion of knotted electromagnetic wave (EMW) in the form of torus knot in a stereographic projection of the field (in the form of electromagnetic soliton) from S^3 locally on the three-dimensional Euclidean space R^3, it is necessary to create a technical transmitting and receiving antennas, it is existing in the space R^3.

The purpose of the experiments prove the existence of knotted EMW induced by this wave of PAR in the Fraunhofer zone at long range radio communication of up to 48 wavelengths $\lambda \sim 13$ cm (6 m), which has an abnormally low attenuation space and time.

The theoretical aspect of the existence of a knotted electromagnetic field is as follows. The experiment is based on the findings of theoretical research of new nontrivial topological solutions of Maxwell's equations written in the second exterior differential forms. It is the existence of electromagnetic field described by these equations, due to the phenomenon of the Hopf bundle [1] S^3 hypersphere physical space (vacuum), where the stereographic projection S^3 parallels in each of its points on our observable 3-dimensional Euclidean space has the shape of knotted 3-tori . meridian lines (circles Villars) these tori set orbit of U(1) symmetry of the interior of the electromagnetic field (ie layers of the principal bundle), these lines in the physical dimensions and determine the magnetic field lines and orthogonal electric field, and the connection of the principal bundle determines intensity physical fields. In fact, these knotted tori (torus knots or mnogolistnika) lines of force of electromagnetic fields and are the above topological solution of Maxwell's equations.

Hopf bundle 2-dimensional sphere S^2 in a 3-dimensional sphere (hypersphere) is considered in the S^3 hmernyh 4-Euclidean space-time R^4 with a map (coordinates)

$h = (\varphi, \theta) = (\varphi (x_1, x_2, x_3. x4 = c \cdot t), \theta (x_1, x_2, x_3, x_4 = c \cdot t)) S^3 \rightarrow S^2$, where c - the light velocity, t -time; φ, θ- orthogonal complex scalar functions.

This 4-dimensional Euclidean space sphere equation

S^3: $x_1^2 + x_2^2 + x_3^2 + x_4^2 = 1$, a (stereo) projective three-dimensional space

$R^3 = \{y_1, y_2, y_3\}$, where $y_i = x_i / (1- x_4)$, wherein x_4-axis time $\cdot$ t in R^4 inverse conversion of R^3 is equal to R^4

$x_i = 2y_i / (\rho + 1)$, $x_4 = (\rho -1) / (\rho + 1)$, $\rho = \Sigma y_i^2$, scalar complex plane (φ, θ) is shown in this map Hopf sphere S2 and the other into an integrated stereographic projection With the plane: $S^2 = R^2 \, U \{\infty\} = C \, U \{\infty\}$. As a result of these two compactifications of complex scalar φ and θ can be interpreted, at any time while displaying maps Hopf $S^3 \rightarrow S^2$, which

can be classified into homotopy classes, characterized value Hopf index n. This bundle Hopf global. Lines level scalar function (φ, θ) by construction coincide with the magnetic and electric lines of force (physical dimensions), each of these lines are marked with an appropriate constant scalar $\varphi = \varphi_0$, $\theta = \theta_0$. Both scalar take the same value at infinity, which is equivalent to the compactification (circuit) 3-space $R^3U\{\infty\}$ in the sphere S^3.

We consider electromagnetic waves, which holds a scalar equation $B \cdot E = 0$, where $B = \mu \cdot H$ - vector of magnetic induction, $\mu = 1$ - the magnetic permeability of vacuum, E-vector of the electric field, this is equal to zero orthogonal vectors B, E, and therefore orthogonal (duality) their level of lines, while on the construction of a scalar field level line tangent vector φ certain functions $B(\varphi)$. and the line of the scalar field level theta of tangent vectors $E(\theta)$ for the initial time $t = 0$ (the analytical calculation of these vectors is described below), i.e. we have the following expression vectors:

$$B(\phi) = B(\phi, 0) = -\frac{a}{\pi} \nabla\bar{\phi} \times \nabla\phi ,$$

$$E(\theta) = E(\theta, 0) = -\frac{a}{\pi} \nabla\theta \times \nabla\bar{\theta}, \quad (1)$$

where a value is used to obtain the correct physical dimensions of induction of the magnetic field B and the electric field strength E. The points on the Riemann sphere S^2 or flea, or homologous Poincare sphere correspond to the hypersphere S^3 after the stereographic projection on R^3 closed in Villars-level line of the circle in the form of linked power lines (for twisted EMW), forming a geodetic meridian 2-dimensional layer of the torus in the S^3, and self-linking field lines form a torus knotted torus as trefoil, cinquefoil, ... multifoil knotted EMW. Property-level geometric lines define precisely the lines of force of the electromagnetic field (up to the physical dimensions of the vectors tangent to it) is due to the important fact that, since the exterior differential 2-form surface S^2 of the element is equal to zero, i.e.

$$d\omega_\phi = 0,\ d\omega_\theta = 0, \quad (2)$$

these forms are closed [2]. Hopf bundle local F^*: $S^3 \to S^2$ essentially becomes a form of external pulling operation ("pullback") transferring the 2-form element surface S^2 and the shape of the exterior differential in S^3 hypersphere. The two-component function F to be used in the operator of pullback

F_φ^*: $S^3 \to S^2$, by definition, has the form $F = (F_1, F_2)$ and with respect to the map for φ is equal to

$$F_\varphi = (F_1, F_2) = = (\bar{\phi}(x_1, x_2, x_3, x_4), \phi\ (x_1, x_2, x_3. x_4)), \quad (3)$$

then pulling F_φ^*: $S^3 \to S^2$ of 2-form ω_φ a single element surface S^2

$\omega_\varphi = du \Lambda d\,\bar{u}\ /(1 + u \cdot \bar{u})$ the function F is equal to:

$$F_\varphi^*\,\omega_\varphi = dF_1 \Lambda\, dF_2 = d \Lambda\, d\,\bar{\phi}/(2\pi \cdot i \cdot (1+\bar{\phi}\cdot\phi\ ))^2 = g_\phi \cdot\, d \Lambda\, d\,\bar{\phi}, \quad (4)$$

where g_φ factor normalization unit module 2-form $dF_1 \Lambda\ dF_2$ and converts it into real numbers is:

$g_\phi = 1/(2\pi \cdot i \cdot (1+\bar{\phi}\cdot\phi\ ))^2$, and the outer product of 1-forms (4), and

is $d\phi = \partial_\mu \phi\ dx^\mu$ and $d\bar{\phi} = \partial_\mu \bar{\phi} dx^\mu$ well

$$d\phi\, \Lambda d\bar{\phi} = g_\phi \cdot \partial_\mu \phi\ dx^\mu\, \Lambda \partial_\upsilon \bar{\phi} dx^\upsilon. \quad (5)$$

According to the commutative operation pulling F^*, using (2) we have

$F_\varphi^* d\omega_\varphi = d(F_\varphi^* \omega_\varphi) = 0$, $F_\theta^* d\omega_\theta = d(F_\theta^* \omega_\theta) = 0$, i.e.

$$d(F_\varphi^* \omega_\varphi) = 0,\ d(F_\theta^* \omega_\theta) = 0, \quad (6)$$

as the exterior differential of the new (pullback in S^3) 2-forms $\Omega^{\phi} = F_{\phi}^{*}\omega_{\phi}$ and $\Omega^{\theta} = F_{\theta}^{*}\omega_{\theta}$ zero, these 2-forms are closed.

Pullback 2-forms Ω^{φ} and Ω^{θ} and expressed in terms of a map of the Hopf bundle $h=(\phi, \theta)= (\phi(x_1, x_2, x_3. x_4= c\cdot t), \theta(x_1, x_2, x_3, x_4= c\cdot t))$ as follows. Of relations (4) it follows that

$$\Omega^{\phi} = dF_1 \Lambda dF_2 = g_{\phi}\cdot \frac{\partial_{\mu}\bar{\phi}\cdot\partial_{\vartheta}\phi - \partial_{\vartheta}\bar{\phi}\cdot\partial_{\mu}\phi}{2\pi\cdot i\cdot\left(1+\bar{\phi}\cdot\phi\right)^2}\cdot\left(dx_{\mu}\wedge dx_{\vartheta}\right), \qquad (7)$$

where "dumb" summation is only ordered indices $\mu <\theta$ = 1 ... 4, and in the numerator are the partial derivatives of the coordinates x_1, x_2, x_3. x_4 then the coordinate components of the 2-form Ω_{φ} equal tensor

$$(\Omega^{\phi})_{\mu\upsilon} = \frac{\partial_{\mu}\bar{\phi}\cdot\partial_{\vartheta}\phi - \partial_{\vartheta}\bar{\phi}\cdot\partial_{\mu}\phi}{2\pi\cdot i\cdot\left(1+\bar{\phi}\cdot\phi\right)^2}. \qquad (8)$$

The stereoscopic 3-space R^3 form is Ω^{φ}

$\Omega^{\phi} = g_{\phi}\cdot \partial_i\phi\ dx^i \Lambda\partial_k\bar{\phi}dx^k = g_{\phi}\cdot [\partial_1\bar{\phi}\cdot\partial_2\phi - \partial_2\bar{\phi}\cdot\partial_1\phi)(dx^1 \Lambda dx^2)+$

$(\partial_1\bar{\phi}\cdot\partial_3\phi - \partial_3\bar{\phi}\cdot\partial_1)(dx^1 \Lambda dx^3) + (\partial_2\bar{\phi}\cdot\partial_3\phi - \partial_5\bar{\phi}\,\partial\phi\cdot\partial_2)(dx^2 \Lambda dx^3)]$,

(with Latin indices i, k = 1 ÷ 3) and dual coordinate basis (dx^1, dx^2, dx^3), is transformed by the operator $*$ - "star Hodga" in polyvector equal to the vector product of the gradients ($\nabla\phi, \nabla\bar{\phi}$) on the coordinate functions ϕ (x_1, x_2, x), $\bar{\phi}(x_1, x_2, x_3)$, i.e.

$* \Omega^{\phi} = g_{\phi}\cdot [\partial_1\bar{\phi}\cdot\partial_2\phi - \partial_2\bar{\phi}\cdot\partial_1\phi)\, dx^3 - (\partial_1\bar{\phi}\cdot\partial_3\phi - \partial_3\bar{\phi}\cdot\partial_1)\, dx^2 +$

$\partial_2\bar{\phi}\cdot\partial_3\phi - \partial_5\bar{\phi}\cdot\partial_2)\, dx^1] =$

$$= g_{\phi}\cdot det\begin{pmatrix} dx^1 & dx^2 & dx^3 \\ \partial_1\bar{\phi} & \partial_2\bar{\phi} & \partial_3\bar{\phi} \\ \partial_1\phi & \partial_2\phi & \partial_3\phi \end{pmatrix} = g_{\phi}\cdot(\nabla\bar{\phi}\times\nabla\phi) = B(\phi), \qquad (9)$$

where polyvector $* \Omega_{\varphi}$ defines a dimensionless geometric vector tangent to the lines of the level maps $\phi(x_1, x_2, x_3)$, i. e. meridians Villars on Hopf torus for this card procrastination. Carrying out similar operations for the 3-dimensional subspace conjugate to dual 2-form map $\theta(x_1, x_2, x_3)$, we obtain the relation of dual-like (9)

$$* \Omega^{\theta} = g_{\theta}\cdot det\begin{pmatrix} dx^1 & dx^2 & dx^3 \\ \partial_1\theta & \partial_2\theta & \partial_3\theta \\ \partial_1\bar{\theta} & \partial_2\bar{\theta} & \partial_3\bar{\theta} \end{pmatrix} = g_{\theta}\cdot(\nabla\theta\times\nabla\bar{\theta}) = E(\theta), \qquad (10)$$

where polyvector Ω_{θ} defines a dimensionless geometric vector tangent lines dual card level $\theta(x_1, x_2, x_3)$, i. e. Villars meridians on the orthogonal Hopf torus with a map $\theta(x_1, x_2, x_3)$ orthogonal to the map $\phi(x_1, x_2, x_3)$, thus the vector of certain fields by construction in (1), comply with the same vector in (9.10) have certain analytically from the geometrical representations up to the physical dimension.

The relationship of these fields (B, E) is a set of Maxwell's equations of the properties of closed 2-forms in (6) that can be represented (by lemma Poincaré) through the differential on the exact 1-forms Ω^{ϕ} and Ω^{θ} some dimensionless vectors, which are defined below:

$J^{\phi} = (J^{\phi}_0, J^{\phi}_1, J^{\phi}_2, J^{\phi}_3)$ and $J^{\theta} = (J^{\theta}_0, J^{\theta}_1, J^{\theta}_2, J^{\theta}_3)$, these 1-forms in 4-dimensional space have the form

$\Omega^{\phi} = J^{\phi}_0\cdot dx_0 + J^{\phi}_1\cdot dx_1 + J^{\phi}_2\cdot dx_2 + J^{\phi}_3\cdot dx_3$

$\Omega^{\theta} = J^{\theta}_0\cdot dx_0 + J^{\theta}_1\cdot dx_1 + J^{\theta}_2\cdot dx_2 + J^{\theta}_3\cdot dx_3$

Vectors J^{φ} and J^{θ} physically dimensional form, for example, multiplied at $a = (h \cdot f /e)$, where h - Planck constant, f-frequency electromagnetic wave,

e - electron charge, equal

$J^{\phi}_{\mu} \cdot (h \cdot f/J) = A^{\phi}_{\mu}$,

$J^{\theta}_{\mu} \cdot (h \cdot f/J) = A^{\theta}_{\mu}$.

They define the classic 4-dimensional vector electromagnetic potentials:

$A^{\phi} = (A^{\phi}_0, A^{\phi}_1, A^{\phi}_2, A^{\phi}_3)$ and $A^{\theta} = (A^{\theta}_0, A^{\theta}_1, A^{\theta}_2, A^{\theta}_3)$, (11)

1-forms on which respectively A^{φ} and A^{θ}:

$A^{\phi} = A^{\phi}_0 \cdot dx_0 + A^{\phi}_1 \cdot dx_1 + A^{\phi}_2 \cdot dx_2 + A^{\phi}_3 \cdot dx_3 = A^{\phi}_{\mu} \cdot dx^{\mu}$

$A^{\theta} = A^{\theta}_0 \cdot dx_0 + A^{\theta}_1 \cdot dx_1 + A^{\theta}_2 \cdot dx_2 + A^{\theta}_3 \cdot dx_3 = A^{\theta}_{\mu} \cdot dx^{\mu}$. (12)

The second form of the 1-forms and Aφ Aθ as external differentials of them are

$dA^{\phi} = (\partial_{\mu} A^{\phi}_{\upsilon} - \partial_{\upsilon} A^{\phi}_{\mu})\ (dx^{\mu} \Lambda\ dx^{\upsilon})$, (13)

where the coefficients of these two forms of electromagnetic fields are the components of the electromagnetic field tensor have the form:

$\Phi_{\mu\upsilon} = \partial_{\mu} A^{\phi}_{\upsilon} - \partial_{\upsilon} A^{\phi}_{\mu}$, (14)

For example, in (1) the components of the magnetic induction vector in the map

$B_j = -1/2 \cdot e_{ikj}\ G_{\phi} \cdot \partial_i \bar{\phi} \cdot \partial_k \phi - \partial_k \bar{\phi} \cdot \partial_i \phi$), (15)

they are the same, but expressed in terms of the tensor Φ^{ik} in dual map θ equal to

$B_j(\theta) = -1/2 \cdot e_{ikj} \cdot \Phi^{ik}(\theta) = -(B_1(\theta)\ \ B_2(\theta)\ \ B_3(\theta))$. (16)

Taking the exterior differential of (12) and (13), we obtain the second exterior differentials:

$ddA^{\phi} = d^2 A^{\phi} = 0$,

$ddA^{\theta} = d^2 A^{\theta} = 0$, (17)

on the property of the second external differential equal to zero from any external form.

In fact, the system of external forms in (17) is Maxwell's equations in external forms. Exploded their record, expressed in terms of the intensity of the electromagnetic field tensor in (14), is as follows: the first pair of Maxwell's equations in coordinate form is:

$e^{\mu\vartheta\gamma\delta} \partial_{\vartheta} \Phi_{\gamma\delta}(\phi) = \partial_{\vartheta} {}^{*}\Phi^{\mu\vartheta}(\theta) = 0$, where ${}^{*}\Phi_{\gamma\delta}(\theta)$ -dual tensor

$e^{\mu\vartheta\gamma\delta} \partial_{\vartheta} \Phi_{\gamma\delta}(\theta) = \partial_{\vartheta} {}^{*}\Phi^{\mu\vartheta}(\phi) = 0$, (18)

the second pair of Maxwell's equations is

$\partial_{\vartheta} \Phi^{\vartheta\delta}(\phi) = 0$,

$\partial_{\vartheta} \Phi^{\vartheta\delta}(\theta) = 0$, (19)

where the matrix eαβμν an absolutely antisymmetric unit pseudotensor -4th grade. Briefly, tensor equations of Maxwell (16, 17) in the external forms have the form:

The first pair $d^{*}\Phi\ (\phi) = 0$, $d^{*}\Phi\ (\theta) = 0$,

the second pair $d\Phi\ (\phi) = 0$, $d\Phi\ (\theta) = 0$.

Equations (15) and (16) for the magnetic field:

$\boldsymbol{G_{\phi} \cdot (\partial_i \bar{\Phi} \cdot \partial_k \phi - \partial_k \bar{\Phi} \cdot \partial_i \phi) = \Phi^{ik}(\theta)}$, (20)

The equations similar (20), but for the electric field in (1) by changing $\phi \to \theta \to \phi$ in (18÷20), define a system of nonlinear partial differential equations of second order with respect to unknown cards Hopf transformation φ, θ, solved the initial data of the Cauchy.

The meaning of (20) is as follows. The essence of the engaged and knotted the electromagnetic field is described on one side observable physical tensor of the electromagnetic field, and on the other hand, this is the essence defined a geometric object as a Hopf transformation maps gradients as homotopy sphere map the S^2, for instance Poincaré (Bloch), the scope of Stokes -antistoksovyh settings flat polarization of the electromagnetic field in the sphere of non-Euclidean space S^3. It is a space S^3 is real, but it is observed in the stereographic projection S3 to our Euclidean space R^3 in the form of Hopf tori (ie swollen circles of latitude of the sphere S3). These tori meridian (circle Villars) coincides with the line of force of the magnetic and electric components of the electromagnetic field. That is, this field renders (by pulling the differential 2-forms) geometric layers on the torus Hopf bundle and meridians in the physical dimensions of the power lines on the torus are the physical layer of the Hopf bundle, the same meridians layer are orbits Abelian symmetry group U (1) is an electromagnetic field. And homotopy symmetry is not a trivial bundle $h^*: S^3 \to S^2$ has a fundamental loop groups π: equal to Z - infinite natural number of S^3 turns around the sphere S^2 along these orbits (meridians of the torus) Lie group.

Thus the geometric topology of the space defined by the existence of a physical field with accuracy to the physical dimension.

The decision to engage and knotted the electromagnetic fields in a bundle Hopf space.

As to solve the system (18, 19, 20) of non-linear equations in the Hopf map (φ, θ) functions generally difficult [2], the particular solution constructed as a first approximation. That is, the relation (20) is considered as a system of equations known to the right part of the tensor of the electromagnetic field in the form of a sinusoidal excitation function in time and space, i.e. as running along the axis of the torus Z = x3 monochromatic plane wave of linear polarization with the appropriate Stokes component on the sphere S2, then in the first approximation function Hopf map φ (x, t) is of non-linear partial differential equations of the first order of standard type for the motion of the front coming and outgoing (±) inhomogeneous (toroidal knotted) and monochromatic (wideband frequency - impulse) wave:

$$\partial_0\bar{\phi} \cdot \partial_3\phi - \partial_3\bar{\phi}\cdot\partial_0\phi = \sin(\omega t \pm kx), \qquad (21)$$

that is, the right side of the equations (20, 21) is seen as forcing "field strength" of the dynamical equations. As

$\phi = \alpha + i\beta$, $\bar{\Phi} = \alpha - i\beta$, that

$$\partial_0(\alpha - i\beta)\cdot \partial_3(\alpha+i\beta) - \partial_3(\alpha - i\beta)\cdot\partial_0(\alpha+i\beta) = \sin(\omega t \pm kx), \qquad (22)$$

For brevity, we use "silent" partial designation, i. e.

$$\partial_0(\alpha - i\beta) = (\alpha - i\beta)_{,0} = \alpha_{,0} - i\beta_{,0}$$

$$\partial_3(\alpha+i\beta)=(\alpha+i\beta)_{,3}=\alpha_{,3}+i\beta_{,3}\ . \qquad (23)$$

In view of (23) instead of (21, 22) have

$$\alpha_{,0}\cdot\alpha_{,3} + i\alpha_{,0}\cdot\beta_{,3} - i\alpha_{,3}\cdot\beta_{,0} + \beta_{,0}\cdot\beta_{,3} - \alpha_{,3}\cdot\alpha_{,0} - i\,\alpha_{,3}\cdot\beta_{,0} + i\beta_{,3}\cdot\alpha_{,0} - \beta_{,3}\cdot\beta_{,0} = \sin(\omega t \pm kx) \qquad (24)$$

or

$$2i(\alpha_{,0}\cdot\beta_{,3} - \alpha_{,3}\cdot\beta_{,0}) = \sin(\omega t \pm kx). \qquad (25)$$

Using the Cauchy-Riemann conditions for complex variables
$\alpha_{,0}= \beta_{,3}$ $\beta_{,0}= -\alpha_{,3}$, equation (25) takes the form
$2i(\alpha_{,0}\cdot \alpha_{,0}+\alpha_{,3}\cdot \alpha_{,3}) = sin(\omega t\pm kx)$ or
$2i(\alpha_{,0}^2+\alpha_{,3}^2)= sin(\omega t\pm kx)$ 26)
Similarly for $\beta_{,0}$, $\beta_{,3}$
$2i(\beta_{,0}^2+\beta_{,3}^2)=sin(\omega t\pm kx)$ (27)
Taking into account the normalizing factor in (20) we have
$(\alpha_{,0}^2+\alpha_{,3}^2) = \pi(1+\bar{\phi}\cdot\phi))^2 sin(\omega t\pm kx)= \pi(1+ \alpha^2 + \beta^2)^2 sin(\omega t\pm kx)$
$(\beta_{,0}^2+ \beta_{,3}^2) = \pi(1+\bar{\phi}\cdot\phi))^2 sin(\omega\pm kx)= \pi(1+ \alpha^2 + \beta^2)^2 sin(\omega t\pm kx)$,
where the physical dimension of the factor is omitted.

We consider the motion of the waves near the beginning of the stereographic projection about anti polar point of S^3 with zero initial Cauchy conditions, so for all the quantities are small compared with unity (S^3 sphere of radius), and the value of α, β are small compared with unity, i. e., $\alpha^2 + \beta^2 \sim 0$ and $\bar{\phi}\cdot\phi \sim 0$ in the Normalizing Multiplier, then we have
$(\alpha_{,0}^2+\alpha_{,3}^2) \approx \pi\cdot sin(\omega t\pm kx)$
$(\beta_{,0}^2+\beta_{,3}^2)\approx \pi\cdot sin(\omega t\pm kx)$. (28)

The solution of equations (28) for modules of the vectors B and E (1) standard [3] - exists only for the positive half cycle of the sine and has the form:

$$\alpha= \beta= \int_0^{x_0} \sqrt{\frac{1}{\left(\frac{\omega}{c}\right)^2 + k^2}\sin\left(\frac{\omega x_0}{c} \pm kx_3\right) + C_1}\, d\left(\frac{\omega x_0}{c} + kx_3\right)+C_2, \quad (29)$$

with zero initial Cauchy conditions instead of (29) we have

$$\alpha= \beta= \omega \int_0^{x_0} \sqrt{\frac{1}{\left(\frac{\omega}{c}\right)^2 + k^2}\sin(\omega t \pm kx_3)}\, dt + k \int_0^{x_0} \sqrt{\frac{1}{\left(\frac{\omega}{c}\right)^2 + k^2}\sin(\omega t \pm kx_3)}\, dx_3, \quad (30)$$

$$\alpha=\beta= C \cdot \int_0^{x_0} \sqrt{\sin(\omega t \pm kx_3)}\, dt + \int_0^{x_0} \sqrt{\sin(\omega t \pm kx_3)}\, dx_3 . \quad (31)$$

where the angular frequency $\omega = 2\pi \cdot f$, and the wavelength of the electromagnetic $\lambda = C / f$ - C-the speed of light in vacuum.

Solution integrals in (30, 31) is in the form of incomplete elliptic integral of the second kind, i.e.

$\alpha=\beta=-4E((\pm 2)$ (32)

is a quasi-periodic function automorphic with linearly increasing term. However, the vector of magnetic induction and electric field gradients are determined by the scalar fields (electromagnetic field tensor), and therefore (32) has only informative value, and for practical purposes are required gradients, so the magnetic induction vector in (1)

$$\partial_0\alpha=\partial_3\alpha=\sqrt{\sin(\omega t \pm kx_3)},$$
$$\partial_0\beta=\partial_3\beta=\sqrt{\sin(\omega t \pm kx_3)}, \quad (33)$$

to tension the electric field vector in (1) is similar to (33) are calculated gradients of complex scalar θ:

$\theta= \gamma + i\delta$, $\bar{\theta}= \gamma - i\delta$
$\partial_0\gamma=\partial_3\gamma =\sqrt{\sin(\omega t \pm kx_3)}$,

$$\partial_0\delta=\partial_3\delta=\sqrt{\sin(\omega t \pm kx_3)}. \quad (34)$$

It is a form of a half-wave sinusoidal voltage over the space used in the experiment to excite knotted antennae.

It is important to note that the function has an impulse shape in view graphics modules vectors | *B* | and | *E* | Fig. 1.

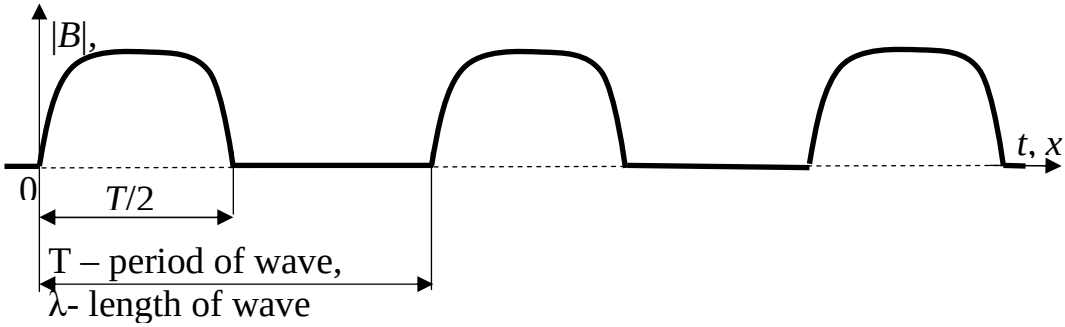

Fig. 1 Schedule UWB pulse electromagnetic wave propagation knotted in the form of a photon-soliton

In accordance with the function (34) the nature of distribution in space and time is an ultra-wideband pulse modulation signal carrier frequency without filling, which is observed in the experiment. The electromagnetic field is concentrated in the assembly form the soliton pulse, nonspreading in space-time. That is, when distributing a pulse S^3 at a stereoscopic R^3 dispersion in space and time of the signal (node) is absent, i.e. it is a photon-soliton is described by a nonlinear differential equation (28). site energy is concentrated in the field of topological soliton, in the form of a trefoil knot tightened (no gaps) lines of magnetic and electric fields.

When moving (rolling) pulse-soliton in the form of a knotted torus along its axis, which takes place along the meridians S^3 hypersphere (straight lines in the stereographic projection in the 3-dimensional Euclidean space) is formed twisted beam of electromagnetic waves (EMW) radiation, the beam is unwrap the tangent lines of force in the form of a toric mnogolistnika topological braids twisted beams (tangent vectors Poynting) emanating from the plane of each loop of the mnogolistnika. The planes of the loops form a helical wave fronts knotted, and normal to the front to form a spiral twisted helix of electromagnetic wave with a nonzero spin and orbital angular momentum. Interwoven spiral (Poynting vector tangent) and materialize the above topological plait solutions of Maxwell's equations.

For the experiment, it is important that the effect described by the geometry of the initial conditions of the Cauchy equations of Maxwell fiber space S3 at the time of excitation braids knotted EMW determined precisely on the surface of knotted antennae, shape and size of the loops which in the form of cinquefoil must match the size and shape of the loop torus knot knotted EMW at each time (this node determines the movement of the time course of the phenomenon).

If cinquefoil loops have identical configuration, the axis of the braid straight, otherwise the radiating loop dephase in space-time and the axis of the braid is bent in space-time in the form of field intensity of the beat.

Technologically, it was difficult to create an identical configuration of the loop, so the radiation axis (braids) vaguely curved in space and time, and it was necessary to adjust the transmit phased array and the receiving PAA by their linear and angular relative movement in space so that radiation spit spiral PAR and spirals partial radiation loops FAR elements as much as possible aligned in space, then the observed maximum signal for each radio distance, which was the main difficulty of the experiment.

To realize this purpose the transmission of PAR and similar reception PAA was established, as well as the stand on which were placed the FAS in the field anechoic conditions. A typical design of phased array element in the form of cinquefoil is described in [4 ÷ 7], which shows more antennas in the form of a trefoil and pyatnadtsatilistnika.

The design of the transmitting and receiving phased array shown in the photo in Fig. 2 side view.

Fig. 2 Photo transmitting phased array (left) and receiving phased array (right) tilt-shift devices pyatilistnikovyh elements as antennas.

Each element of the PAR with the overall diameter of 9 cm is made in the form of a cinquefoil of enamelled copper wire 1.25 mm in diameter at the resonant frequency of the loop 2.5 GHz (wavelength λ = 12 cm is the length of one loop cinquefoil), but since this is a phased array retardation FAS system both along the axis and around the axis of PAR, the PAR wave length is reduced by about 5%, so PAR resonance condition is not satisfied at this wavelength, therefore the operating frequency is decreased by this percentage, i.e. to the resonance frequency equal to 2.375 GHz PAR (wavelength in free space of 12.6 cm), and then in the loop cinquefoil slow-PAR system, it will be reduced by the same 5%, ie, up to 12 cm. PAR elements located along the axis of the exciting rod at a distance of ~

0,5λ = 6,3 cm, so the transverse component of the electromagnetic wave (EMW) of each phased array element is excited in opposite along the axis of the rod, so interferometry extinguished in the wave zone in the direction of perpendicular to the axis, and the longitudinal components are knotted EMW each item, on the contrary, develop in the direction of the axis of the field strength, with the degree of knotting increases multiplicatively, ie in 5x5 = 25 times and corresponds to one dvadtsatipyatilistniku.

The transmission of PAR are cinquefoil right winding (right helicity), and receiving phased array - the left winding (left helicity) to match the helicity ray radiation loops cinquefoil and AFD, as the radiation axis of the transmitting and receiving PAR opposite direction. The exact length of the rod along the axis of symmetry of the FAR, the exciting and stabilizer assembly lines of force of the field, which is equal to ~ λ / 2 = 6.3 cm (chosen experimentally for minimum VSWR), and is excited by the rod with one end connected in series half-wave vibrator (λ / 2 = 6.3 cm) with a balun and matching U-bend on the 50 ohm cable, the other end of the rod is radiating knotted EMW. The total length of the rod ~ 12.6 cm.

The stand is created by dielectric non-reflective structure consisting of guide length of 6 m, the transmitting and receiving mast height of 3 m, the dielectric 2 Degree Swivel device with sliding-lever mechanism, 2-Degree Swivel device from the organic polycarbonate glass, 4-power law tilt-shift tables of Plexiglas to place on their transmitting and receiving phased arrays. Rotary device mounted with FAS in the process of signal attenuation measurements are shown in Fig. 3. It should be noted that the whole structure without metallic fasteners assembled: glue and dielectric pins. For communication antennas measuring device uses radio frequency transmission path cable type RG-58 6 m long with connector N-type (male) and the same type of cable reception path length of 14 m.

Fig. 3 Photos placing the transmission (left) and receiving phased array (to the right) masts in the rotary devices.

The measuring equipment and is compact Vector Network Analyzer (VNA) N9918A-type chains (Field Fox) to 18 GHz company KeySight Technology (USA).

The need to create a stand for measuring the attenuation of long range radio communication of up to 48 wavelengths is that previous results described in [2 ÷ 5], refer to the initial values of the wave Fraunhofer zone of up to 15 wavelengths for axial PAR 5% influence reactivity not near wave zone. Therefore, to achieve greater reliability in terms of the exceptions to the near zones of influence and said anechoic stand was established. Measurement of external signals reflected spent using the transmitting and receiving half-wave dipoles showed no reflection to the level of noise VNA -95 dBm.

The methodology of the experiment was that the initial installation space for PAR on vertical masts were adjusted by a laser beam at a certain distance radio communication multiple of two: L = 3λ, 6λ, 12λ, 24λ, 48λ (6 m), to be fixed in space, a straight line of an electromagnetic beam laser. Next to these places were established FAR and their axes are directed along these lines, then fed to the transmit phased array microwave signal generation output network analyzer, and it was fed to the input signal from the receiving PAA. At each distance communication was carried out by measuring the signal per unit length attenuation at the maximum signal shifts PAR within λ / 2, by the shift of PAR in swing-shift device mast and tilt the entire receiving mast with respect to the vertical. Experimentally, it was found that the radiation spread EMW knotted line is not a straight line, defined during adjustment, but a divergent spiral (helicoid) topological braids. The maximum slope of the receiving mast with respect to the vertical transmission of the mast is about 30, while the spit PAR radiation transmitting coil as possible combined with a spiral braid transmitting phased array radio communication at all distances. It is for these provisions of the transmission of PAR on these distances were recorded radio graphs of signal attenuation in the frequency band of the existence knotted EMW.

During calibration of the measuring system it is established that the level of total losses in the channel of the transmitting and receiving cable length of 20 m is -11dBm, in addition there are losses in the excitation of the transverse component of EMW excited orthogonal axis PAR. The average level of total losses in the cable and losses on the excitation of the transverse components of the electromagnetic wave in a knotted band 2,25 ÷ 2,45 GHz existence longitudinal component knotted EMW is -48 dBm, this amount should be subtracted from all subsequent plots to get the value of it attenuation signal. The frequency of the label "2" 2.326 GHz corresponds to a wavelength of about 13 cm.

First, we measured the per unit length attenuation of the longitudinal component knotted EMW on radio distance 37, 5 cm (about 3 wavelengths ~ 3λ, ie wave Fresnel zone), the measurement result is shown in the graph of Fig. 4. And used the averaging mode (accumulation) 100 Scan Rate (Avg 100 display screen on the photo to the left).

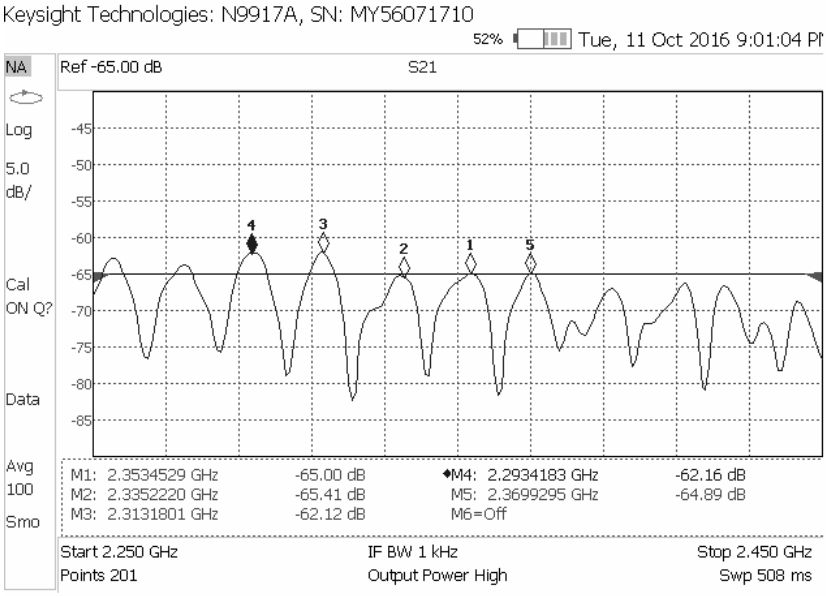

Fig. 4 Schedule damping longitudinal component knotted EMW on radio distance 37, 5 cm (about 3 wavelengths ~ 3λ, ie wave Fresnel zone).

The graph shows that the average loss is equal to -63 dBm and minimum losses on the mark "3" -62.12 dBm, while net losses in the cables and the excitation of the transverse component of the EME average specific (per unit length) attenuation is equal to -15 dBm. Since PAR radiates in both directions, the loss per unit length in one direction are -12 dBm. Then conducted attenuation measurement on radio twice the distance of 75 cm (approximately ~ 6λ) at the beginning of the wave of the Fraunhofer zone) measurement result is shown in Fig. 5.

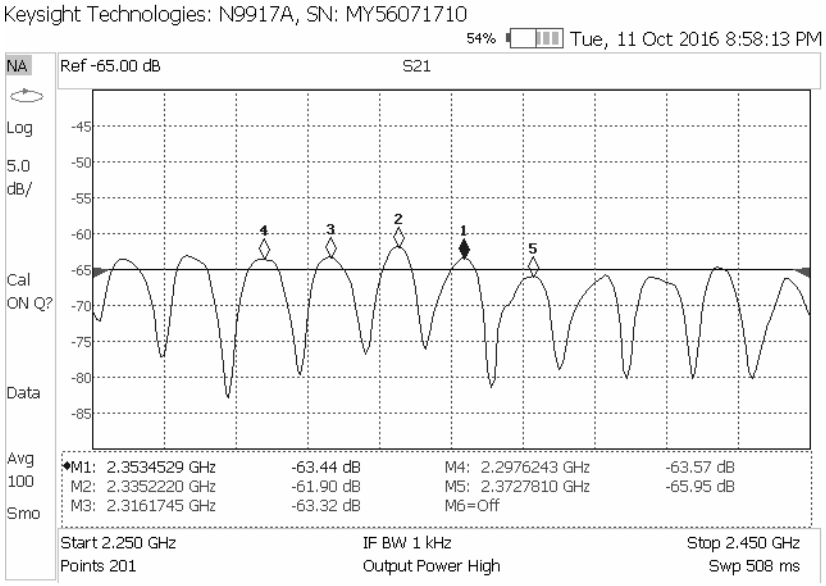

Fig. 5 Schedule damping longitudinal component knotted EMW on the radio distance of 75 cm (about 6 and a wavelength ~ 6λ, ie at the beginning of the wave Fraunhofer zone).

The graph shows that the average loss is equal to -63.6 dBm, and the minimum loss of the label «3» -61,9 ≈ -62 dBm, while the average level of specific attenuation -15.6 dBm.

The result of measurement on radio twice the distance of 150 cm (about ~ 12λ) is shown in Fig. 6.

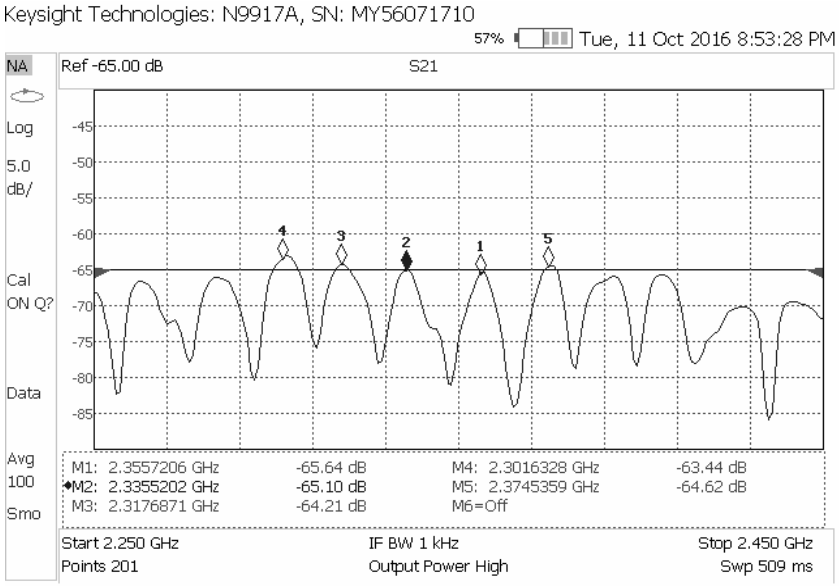

Fig. 6 Schedule 6 damping the longitudinal component knotted EMW on the radio distance of 150 cm (about 12-wavelength ~ 12λ, i. e. at the beginning of the wave Fraunhofer zone).

The graph shows that the average loss is equal to -64.6 dBm and minimum losses on the mark "4" -63.44 dBm, while the average level of specific attenuation -16.6 dBm.

The next measurement is performed on the radio distance of 3 m (about 24 wavelengths ~ 24λ), the measurement result is shown in Fig. 7.

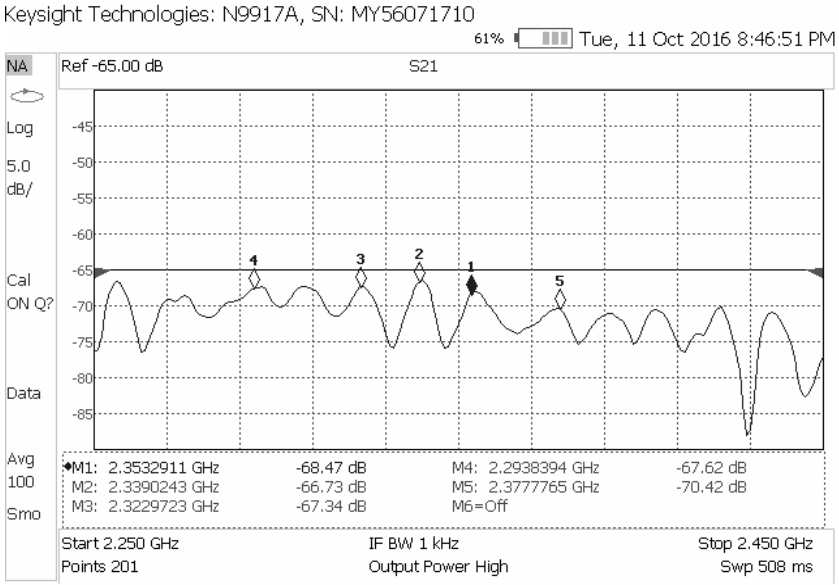

Figure 7. Graph of attenuation of the longitudinal component knotted EMW on the radio distance of 3 m (about 24 wavelengths ~ 24λ, i. e. wave Fraunhofer zone).

The graph shows that the average loss is equal to -67.5 dBm and minimum losses on the mark "2" -66.73 dBm, while the average level of specific attenuation -19.5 dBm.

The last measurement was performed on the radio twice the distance of 6 meters (about 48 wavelengths ~ 48λ), the measurement result is shown in Fig. 8.

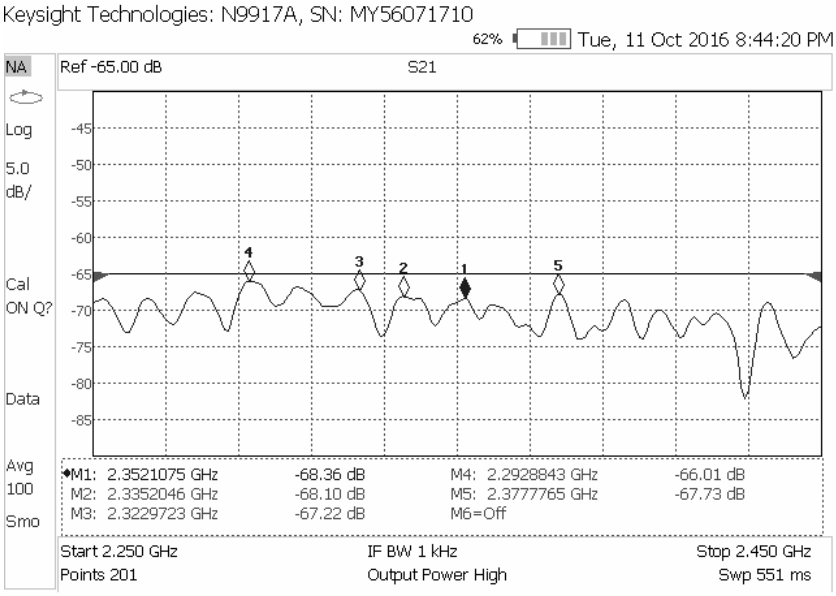

Figure 8. Schedule damping longitudinal component knotted EMW on the radio distance of 6 m (about 48 and wavelength ~ 48λ, i. e. wave Fraunhofer zone).

The graph shows that the average loss is equal to -67.5 dBm and minimum losses on the mark "4" -66.01 dBm, while the average level of specific attenuation -19.5 dBm. From a comparison with the result in the graph in Fig. 7, that should be the average rate level of specific attenuation is almost zero by doubling the distance radio communication with the 3 m to 6 m with an error measuring device 0.4 dBm. It should be noted that the rate of specific attenuation of the transverse electromagnetic wave is equal to -6 dB by doubling the distance radio communication.

Dips in the charts due to the influence of damping resonance harmonics slowing PAR systems.

For reliability was performed 10 more repeated series of measurements over a distance interval along the guide stand equal L≈11 cm step spiral helix radiation cinquefoil each loop, where the average total loss was equal -50 dBm, this value is subtracted from the measured attenuation at all distances radio.

Integral specific attenuation graph of the EMW knotted at different distances radio is shown in Fig. 9.

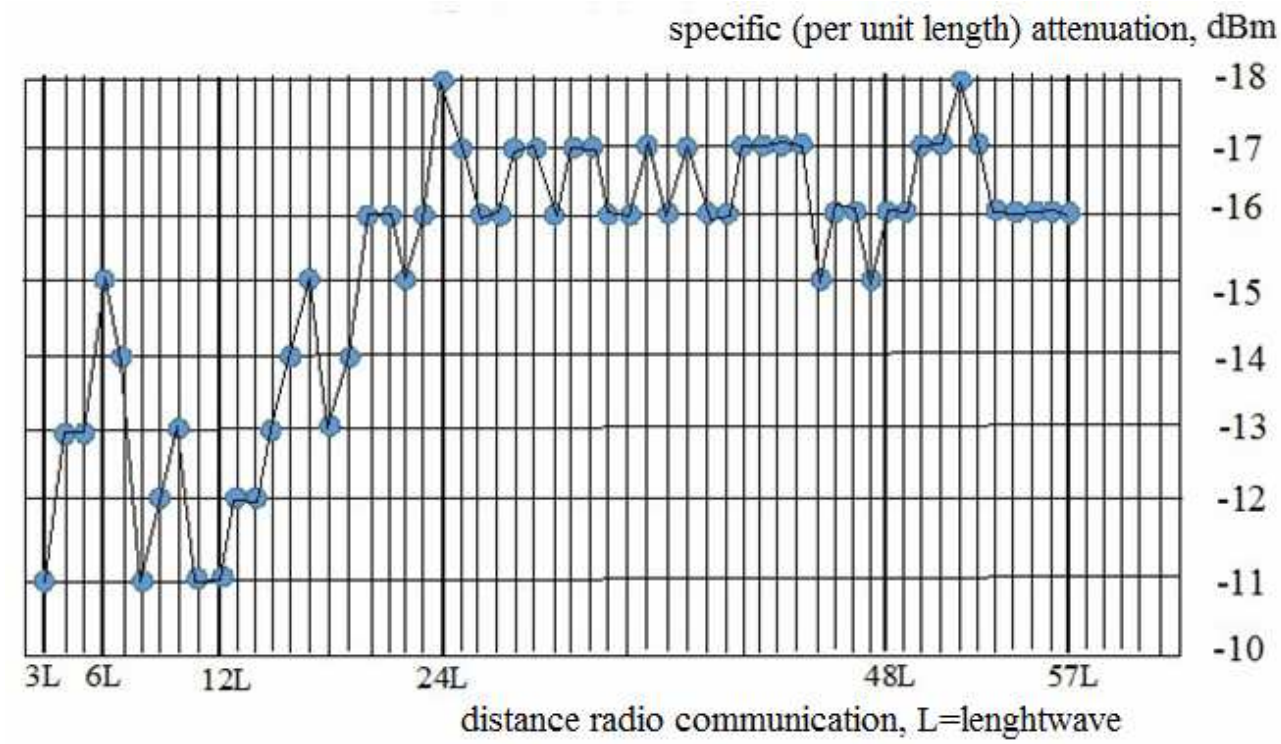

Fig. 9 Schedule attenuation. The circles marked reference.
Step spiral helix L≈ 11 cm.

The observed oscillations of the graph in Fig. 9 due to helicity of the radiation beams each loop cinquefoil PAR. The diameter of the spirals of each loop in a radiation spit is equal to about 2 cm (considering the wavelength λ = 13 cm along the spiral and helical pitch L≈11sm). That is, the radiation propagates in a tube of diameter, in addition, it follows from the exact solutions of nonlinear (soliton) of differential Hopf equations for the electromagnetic field in S3 hypersphere, the diameter of the tube with the distance narrows exponentially, so the total energy of the radiation along the meridian around the sphere S3 is finite and equal to the energy expended in the excitation of the transmitting antenna knotted EMW. Oscillations are important in the transition of the wave Fresnel field (3L ÷ 12L), and the specific attenuation curve is stabilized at the beginning of the wave zone Fraunhofer (12L ÷ 24L) for axial adjustment. Next on the schedule of the curve observed stable almost periodic oscillations specific attenuation due to radiation twisted helicoidal within ± 0,5 dBm relative value of -16.5 dBm. Therefore, the rate of the specific attenuation is 0.5 dBm and at a distance of ≥ 48L the rate of the specific attenuation tends to zero throughout the meridian of the sphere S^3, ie, formed a string of final energy cosmic virtual photons knotted solitons in the form of new solutions of these differential Hopf equations applied to Maxwell's equations

CONCLUSION

From the results of theoretical studies have established that a hypersphere S^3 topology Hopf fiber bundle determines the existence of knotted electromagnetic waves in it. Built a particular solution of the nonlinear differential Hopf equation determining the fiber bundle map, and this map corresponding distribution of lines of force of the electric and magnetic field of the wave. View of the decision in the form of stable (non-dispersive) periodic motions clots wave of electromagnetic energy (soliton-photon) allowed to create

a technical device in a knotted antenna that generates an electromagnetic wave knotted that it is important to carry out experiments to prove the reality of this wave.

From the results of experiments to prove the reality of knotted electromagnetic wave, carried out at various distances radio, it found that near the beginning of the wave zone Fraunhofer 12L ÷ 23L (where L≈11 see step spiral helix) change in the average level of specific attenuation is approximately equal to 0.5 dB, however, for the distance radio from 24L to 57L there is almost zero change in the average specific attenuation (attenuation tempo) that is within the error of the network analyzer to be 0.4 dB. Therefore, thanks to found a reversal of about 3° receiving mast with respect to the transmission mast achieved coincidence spiral (helix) knotted the receiving and transmitting antennas as part of PAR, which ensured the achievement of minimal running losses knotted the longitudinal component of the EMW and achieving near-zero the rate of specific attenuation, but it is more correct to say, that the rate of specific attenuation (attenuation tempo) tends to zero with increasing distance communication along the meridian on the sphere S^3 fiber space radius of ~ 53 billion. light-years. Radiation pattern knotted EMW shrinks with increasing distance radio communication. It should be recalled that the attenuation tempo of the transverse electromagnetic wave is equal to 6 dB when doubling the distance of communication and, on the contrary, expands directional diagram. Q.E.D.

The studies were conducted in collaboration with the Foundation for promising technologies and innovations (Executive Director Tatur V.U.) in the framework of "new physical principles of electromagnetic coupling," and with the assistance of "KeySight TechnologiJs" (USA), granted a precision radio-measuring equipment.

LITERATURE

1. A. F. Ranada, J. L. Trueba Topological electroma gnetism with hidden nonlinearity. Collection: Modern nonlinear optics Part 3. Second Edition Advances in chemical physics. Volume 119. 2001 John Wiley & Sons, Inc. ISBNs: 0-471-38932-3 (Hardback); 0-471-23149-5 (Electronic), p 197.

2. A.F.Ranada. Knotted solutions of the Maxwell equation in vacuum. Journal of Physics A 23, I.815-L.820, 1990.

3. V.F. Zaitsev, F.D. Polyanin. Handbook of differential equations in partial derivatives. M .: 2003

4. Nefedov E.I., Ermolaev Y.M., Smelov M.V. Experimental study of excitation and propagation of electromagnetic waves knotted in different environments. M .: Radio engineering, number 2, 2013, p. 31.

5. Smelov M.V. Experimental study of superluminal propagation velocity knotted electromagnetic waves in a vacuum. M .: Radio engineering, number 1, 2015, p. 70.

6. M.V. Smelov Experimental study of knotted antennae in the form of a trefoil and cinquefoil. M .: Radio engineering, number 2, 2013, p. 23.

7. M.V. Smelov Experimental study of phased antenna array of four antennas in the form of knotted pyatnadtsatilistnikov. M .: Antennas, vol. 9 (208), 2014, p. 18.